Hindawi
Advances in Civil Engineering
Volume 2019, Article ID 3725373, 18 pages
https://doi.org/10.1155/2019/3725373

Research Article

Research on Improved Equivalent Diagonal Strut Model for Masonry-Infilled RC Frame with Flexible Connection

Guang Yang,[1,2,3] **Erfeng Zhao**,[1,2] **Xiaoya Li**,[4] **Emad Norouzzadeh Tochaei**,[5] **Kan Kan**,[2] **and Wei Zhang**[2,6]

[1]*State Key Laboratory of Hydrology-Water Resources and Hydraulic Engineering, Hohai University, Nanjing 210098, China*
[2]*College of Water Conservancy and Hydropower Engineering, Hohai University, Nanjing 210098, China*
[3]*National Engineering Research Center of Water Resources Efficient Utilization and Engineering Safety, Hohai University, Nanjing 210098, China*
[4]*Melbourne Business School, The University of Melbourne, Parkville, VIC 3010, Australia*
[5]*Civil and Materials Engineering, University of Illinois at Chicago, 842 W Taylor St., Chicago, IL 60607, USA*
[6]*The Water Conservancy Bureau of Yangzhou, Yangzhou 225000, China*

Correspondence should be addressed to Guang Yang; 920764311@qq.com and Erfeng Zhao; zhaoerfeng@hhu.edu.cn

Received 25 October 2018; Revised 6 January 2019; Accepted 4 February 2019; Published 4 March 2019

Academic Editor: Chiara Bedon

The reinforced concrete (RC) frame with masonry infill wall is one of the most common structural systems in many countries. It has been widely recognized that the infill wall has significant effects on the seismic performance of RC frame structure. During the Wenchuan earthquake (China 2008), a lot of infilled RC frame structures suffered serious damages due to the detrimental effects brought about by the infill wall rigidly connected to the surrounding frame. In order to solve this problem, flexible connection, introduced by Chinese designers, is recommended by the updated Chinese seismic design code, because of its effect to reduce the unfavorable interaction between infill wall and frame. Although infilled RC frame structure with flexible connection has a lot of advantages, but because of the lack of research, this structure type is seldom used in practical engineering. Therefore, it is of great significance to scientifically investigate and analyze the effects of flexible connection on structure behaviors of infilled RC frame. In this study, a macrofinite element numerical simulation method for infilled RC frame with flexible connection was investigated. Firstly, the effects of connection between infill wall and surrounding frame on in-plane behaviors of infilled RC frame were discussed. Secondly, based on deeply studying the equivalent diagonal strut models for infilled RC frame with rigid connection, an improved equivalent diagonal strut model for infilled RC frame with flexible connection was proposed. Employed with inversion analysis theory, the parameter in the proposed model was estimated through artificial fish swarm algorithm. Finally, applied with the existing experiment results, a case study was conducted to verify the effectiveness and feasibility of the proposed model.

1. Introduction and Literature Review

Infilled reinforced concrete (RC) frame structure is a commonly used structural system around the world. Usually, the infill wall is considered as a nonstructural component, and the interaction between infill wall and surrounding frame is ignored. However, numerous studies have shown that infill wall has significant effects on the seismic performance of RC frame structure. With the deepening of research and complexity, some scholars believed that the connection between infill wall and surrounding frame also has considerable influences on the seismic performance of infilled RC frame. Generally speaking, applied with some construction measures, such as concrete structural column, core columns, binding steel bar, and so on, the infill wall close connects with the surrounding frame. This kind of connection is called rigid connection, as shown in Figure 1(a). However, during the 2008 Wenchuan earthquake, a lot of masonry-infilled RC frame structures suffered severe damages (Figure 2), due to the detrimental

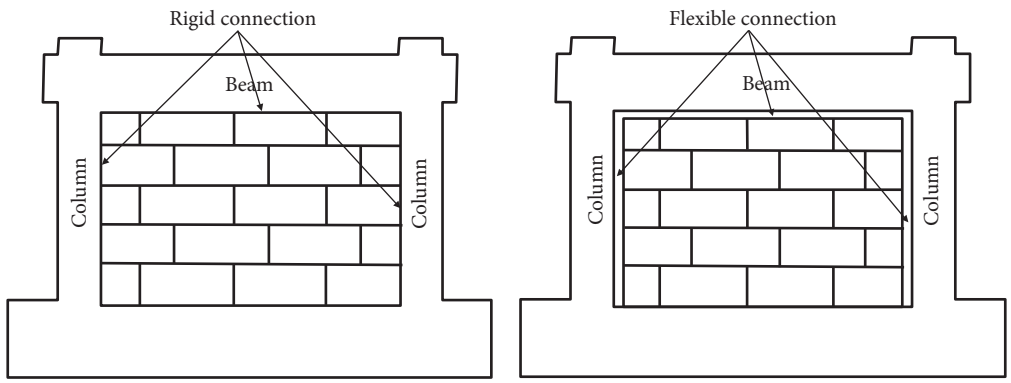

(a) (b)

Figure 1: Connection types between infill wall and surrounding frame.

(a) (b) (c)

(d) (e) (f)

Figure 2: Damages of infilled RC frames after the 2008 Wenchuan earthquake.

effects brought about by the infill wall rigidly connected to the surrounding frame. In order to solve this problem, a preset crack is set between the infill wall and the surrounding frame, and the width of preset crack is in the range of 20 mm~30 mm. Moreover, the preset crack is filled with vibration-absorptive material, such as polystyrene foam board and flexible foaming agent. Therefore, the infill wall is separated from the surrounding frame, and this kind of connection is called flexible connection (Figure 1(b)) by Chinese designers. According to the updated Chinese seismic design code [1], the flexible connection is recommended, because of its ability to reduce the unfavorable interaction between infill wall and surrounding frame as well as to improve the seismic performance of infilled RC frame structure [2]. Therefore, it is of great significance to scientifically investigate and analyze the effects of flexible connection on behaviors of infilled RC frame.

To data, in general, many researchers have experimentally and numerically investigated the structure behaviors of infilled RC frame. Following, an overview of research findings were investigated. Since the first attempt completed by Thomas [3], a large number of experiment researches on infilled RC frame have been concluded. Mehrabi et al. [4] completed an experiment research on twelve RC frames infilled with brick masonry and concluded that the maximum force capacity of infilled RC frame is about 1.5~2.3 times than that of bare frame. Stylianidis [5] introduced three successive experiment studies on RC frame which were infilled with perforated clay brick block masonry. Tests results showed that the effects of infill wall on the strength, stiffness, and energy dissipation capacity of RC frame are significant. The data from Kakaletsis and Karayannis [6] indicated that RC frames with strong infills showed higher initial stiffness and

higher ductility than those with weak infills, but infill strength did not substantially influence strength or energy dissipation. Cavaleri and Trapani [7] reported that the frames infilled with lightweight concrete masonry and calcarenite masonry can improve the dissipative properties compared to the RC frames infilled with clay masonry. Regarding the effects of opening on the performance of infilled RC frame, Kakaletsis and Karayannis [8] investigated single-story, single-bay scaled specimens under cyclic horizontal loading. Research results showed that for low lateral displacement, the energy dissipation of specimens with openings was higher than that of bare frame; for high lateral displacement, the energy dissipation of specimens with openings was reduced and that of the bare frame remained constant. Mallick and Garg [9] investigated the effect of opening positions on the behavior of infilled RC frames with or without shear connectors. They found that an opening at either end of the loaded diagonal of an infilled frame without connectors reduces its lateral strength about 75%, and its lateral stiffness about 85–90% as compared to that of a similar infilled frame with solid infill wall (without opening). For infilled RC frames with shear connectors, the presence of an opening on either end of the loaded diagonal reduces its stiffness by 60%–70% as compared to that of similar infilled RC frame with a solid infill wall. For both types of frames, the loss of strength and stiffness due to a centrally loaded square opening having side dimensions one fifth those of the panel is about 25%–50% compared to similar frames without openings. In recent years, some Chinese researchers considered the effects of connection between infill wall and surrounding frame. Jiang et al. [10] completed an experimental research on five RC frame specimens with masonry infill wall and flexible connection. The results showed that flexible connections can retard the stiffness degradation and improve the energy dissipation ability of frame structure. Zhou et al. [11] and Peng et al. [12] investigated the failure mechanism and seismic behaviors of the infilled RC frames with different connections. The experimental results showed that the specimens with flexible connection have lower bearing capacity than those with rigid connections, but the other performance indexes are better.

In recent years, there have been achieved great successes in nonlinear finite element modeling methods for masonry-infilled RC frame structures [13–19]. From a general point of view, there are two different approaches [20–23]: microfinite element approach and macrofinite element approach, as shown in Figure 3. According to Lourenco [21], the micromodelling approach for masonry infill wall can be summarized in two different ways: simplified micromodelling method and detailed micromodelling method. For the first one (Figure 4(a)), the expanded units are represented by continuum elements and the properties of mortar and brick-mortar interface are lumped into a common element. For the second one (Figure 4(b)), brick units and mortar are represented by continuum elements, and brick units-mortar interaction are represented by different continuum elements, which leads to accurate results and intensive computational requirement. Zhou et al. [24] proposed a microfinite element simulation method for infilled RC frame with flexible connection. The plane stress element was utilized to simulate the infill wall, and the spring element was utilized to simulate the connection between filled wall and surrounding frame. The simulation results showed that the proposed method can reflect the characteristics of wall-frame interactions effectively. Applied with the quasistatic test results, a finite element analysis research was conducted by Peng et al. [12]. Research results showed that the influence of connection type and constructional details of infill wall are significant. Till now, the microfinite element methods for infilled RC frame have achieved a lot of achievements, and extensive and in-depth state-of-the-art reports can be found in [23]. However, studies on the microfinite element methods for infilled RC frame with flexible connection are relatively few.

For macrofinite element method, it is on the basis of replacing the infill wall by one (or more) equivalent strut. This method is usually frequently employed in order to perform nonlinear static or dynamic analyses because of its simplicity, and most technical codes also suggest the macromodel method. Holmes [25] replaced the infill wall with an equivalent diagonal strut, and the cross-section width (w) equal to 1/3 of the diagonal length (d). Afterwards, based on modifying the equivalent width, several researchers put forward a series of detailed methods [26–28]. With the deepening of research and complexity, some researchers took into account the local shear stresses transferred by the infill wall to the surrounding frame and proposed a series of multiple-strut macrofinite element models. Crisafulli [29] investigated the influence of different multiple-strut configurations in structural response. Crisafulli and Carr [30] developed a multiple-strut macrofinite element model including classical truss elements and a special shear spring to simulate the influence of the vertical load on the overall strength of the infill wall (Figure 5(a)). Chrysostomou et al. [31] proposed a six-strut model, which take into account both stiffness and strength degradation of infill walls (Figure 5(b)). El-Dakhakhni et al. [32] proposed a three-strut model having one concentric and two eccentric struts (Figure 5(c)). For infill walls with openings, some researchers have proposed the use of conventional equivalent diagonal struts with a reduction factor, the value of which is derived from some geometrical properties of opening and masonry infill wall [33, 34]. Another approach to model a masonry infill wall with opening is to use a series of horizontal springs, where each spring represents a subpanel of infill wall [35]. Till now, the macrofinite simulation methods for infilled RC frame have achieved considerable success; extensive and in-depth state-of-the-art reports can be found in [36, 37].

Judging from the existing research findings, studies on experiments and numerical simulation methods for infilled RC frame with flexible connection are few, and there is no systematic study. In this study, a macrofinite element numerical simulation method for infilled RC frame with flexible connection was proposed. Firstly, the effects of connection between infill wall and surrounding frame on in-plane

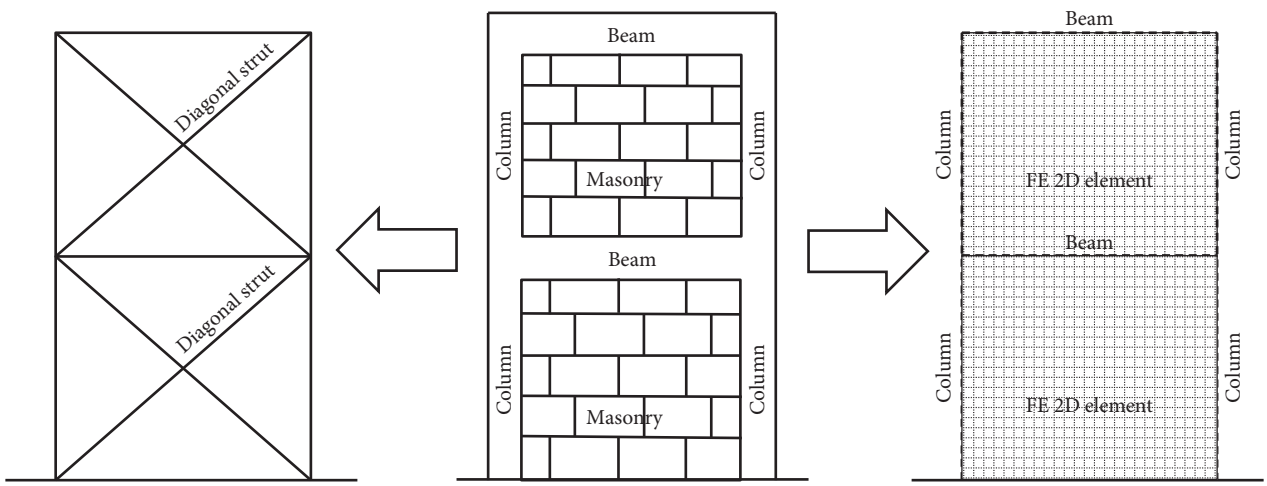

Figure 3: Macrofinite element approach and microfinite element approach.

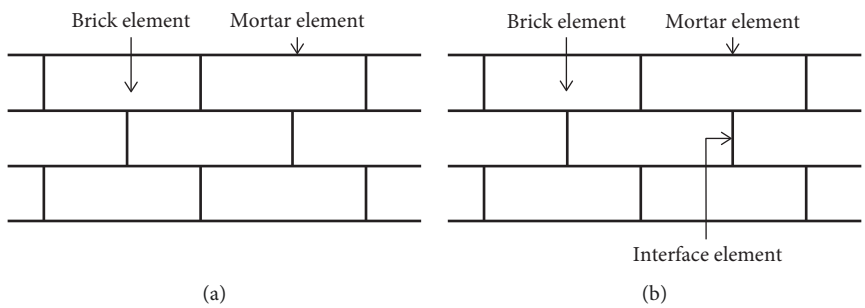

Figure 4: Micromodeling method: (a) simplified micromodeling; (b) detailed micromodeling.

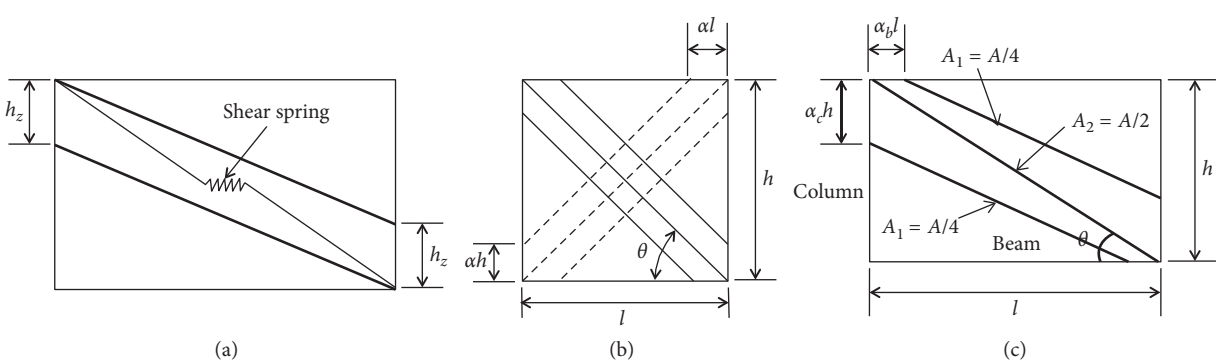

Figure 5: Multiple-strut macrofinite element models: (a) double-strut model with shear spring [30]; (b) six-strut model [31]; (c) three-strut model [32].

behaviors of infilled RC frame were discussed. Secondly, based on deeply studying the equivalent diagonal strut models for infilled RC frame with rigid connection, an improved equivalent diagonal strut model for infilled RC frame with flexible connection was proposed, and the parameter in the proposed model was estimated through artificial fish swarm algorithm. Finally, based on the existing experiment results, a case study was conducted to verify the effectiveness and feasibility of proposed model. Simulation results showed that the proposed model is effective.

2. Effects of Connection on In-Plane Behaviors of Infilled RC Frame

In this section, combined with existing research achievements, the effects of connection between infill wall and surrounding frame on in-plane behaviors of infilled RC frame were deeply discussed, which lays a solid foundation for the subsequent research.

Generally speaking, under the action of horizontal lateral force, the in-plane failure process of infilled RC

frame consists of four stages, and the characteristics in each stage can be characterized as follows. In stage 1, infill wall and surrounding frame are in elastic state and work together to bare the horizontal lateral force. In stage 2, with the increase of lateral load, cracks occur at the contact area of surrounding frame and infill wall, and the diagonal areas of infill wall are crushed. In this stage, the frame structure is still in elastic state, but because of the propagation of concrete cracks and crushed zone, infill wall and surrounding frame cannot work together to bare the horizontal lateral force. In stage 3, with the continuous increase of load, cracks occur at beams and columns, and due to the oversize crushed zone, the infill wall loses its bearing capacity. In stage 4, the horizontal lateral force is mainly borne by beams and columns. When the horizontal lateral force reaches a threshold, the frame structure will be destroyed. From the point of view of lateral deformation, the above-mentioned failure process can be simplified as a deformation process as shown in Figure 6(a). Figure 6(b) shows the stiffness degradation of two specimens performed by Huang [38], one specimen is a bare frame and another one is an infilled RC frame with rigid connection. Figure 6(c) shows the deformation failure processes of above-mentioned two specimens under the action of horizontal lateral forces, and the following conclusions can be obtained. Firstly, the initial lateral stiffness of infilled RC frame with rigid connection is about 2.69 times than that of bare frame. During the experimental process, the stiffness degradation of infilled RC frame with rigid connection is faster than that of bare RC frame. At the end of experiment, the lateral stiffness of infilled RC frame with rigid connection is approximately equal to that of rare frame, which indicates that the infill wall has basically been destroyed in the later stage, and the lateral stiffness of frame structure are mainly provided by frame. Secondly, for the specimen with rigid connection, the yield displacement and yield load are about 7.12 mm~8.03 mm and 169 KN~272 KN, respectively; and for the rare frame, the yield displacement and yield load are about 9.13 mm and 145 KN, respectively. So, the infilled RC frame with rigid connection yielded earlier than the rare frame in the experiment process. Thirdly, the horizontal bearing capacity of infilled RC frame with rigid connection is 271 KN, about 1.6 times that of the bare frame (191 KN). Therefore, infill wall with rigid connection can significantly enhance both the initial lateral stiffness and strength of frame structure, but due to the effects brought about by infill wall rigidly connected to surrounding frame, the infill wall is easy to be damaged under the action of horizontal lateral forces.

In order to investigate the effects of flexible connection on in-plane behaviors of infilled RC frame, a quasistatic experiment was performed by Zhou et al. [11]. Figure 7(a) shows the stiffness degradation of three specimens, one specimen is a rare frame, one is an infilled RC frame with rigid connection, and another one is an infilled RC frame with flexible connection; Figure 7(b) shows the deformation failure processes of above-mentioned specimens; Figure 8 shows the failure modes of above-mentioned specimens; and the following conclusions can be obtained. Firstly, the initial lateral stiffness of infilled RC frame with rigid connection is about 4.28 times that of bare frame, and the initial lateral stiffness of specimen with flexible connection is about 1.96 times that of bare frame. During the experimental process, the stiffness degradation processes of specimens with rigid connection and flexible connection are all faster than that of bare frame, but flexible connection can retard the stiffness degradation of frame structure. Secondly, for the specimen with rigid connection, the yield displacement and yield load are about 6.84 mm and 373.88 KN, respectively; for the specimen with flexible connection, the yield displacement and yield load are about 7.08 mm and 251.0 KN, respectively; and for the rare frame, the yield displacement and yield load are about 9.59 mm and 166.3 KN, respectively. Thirdly, the horizontal bearing capacity of specimen with rigid connection is 421.1 KN, about 1.48 times than that of bare frame (284.5 KN), and the horizontal bearing capacity of specimen with flexible connection is 331.2 KN, about 1.16 times that of the bare frame. According to the above analysis, although the effects of flexible connection on lateral stiffness and bearing capacity of frame structure are inferior to that of rigid connection, it can reduce the unfavorable interaction between infill wall and surrounding frame, retard the stiffness degradation, and effectively improve the seismic performance of frame structure.

3. Improved Equivalent Diagonal Strut Model

According to Section 2, there exist significant differences in effects of connection on in-plane behaviors of infilled RC frame. On this basis, based on discussing the action pattern of flexible connection, an improved equivalent diagonal strut model for simulating the in-plane behavior of infilled RC frame with flexible connection was proposed in this section.

3.1. Action Pattern of Flexible Connection. The infilled RC frame with flexible connection is one kind of new structure types, so there are great differences between the action pattern of flexible connection and that of rigid connection. Generally speaking, the action pattern of rigid connection can be characterized by contact model, as shown in Figure 9(a). Specifically, in normal direction, if contact pressure is less than or equal to 0, two contact surfaces will separate from each other, and if contact pressure is greater than 0, load will transfer between infill wall and surrounding frame. For flexible connection, the preset crack between infill wall and surrounding frame is filled with vibration-absorptive materials, so its action pattern is much more complicated than that of rigid connection. Based on deeply studying the properties of vibration-absorptive materials [39, 40], the compression behavior of filling material can be characterized by the Kelvin model [41, 42] and the tensile behavior of filling material can be characterized by failure element model [42], as shown in Figure 9(b). Therefore, if the microfinite element analysis approach is adopted, the

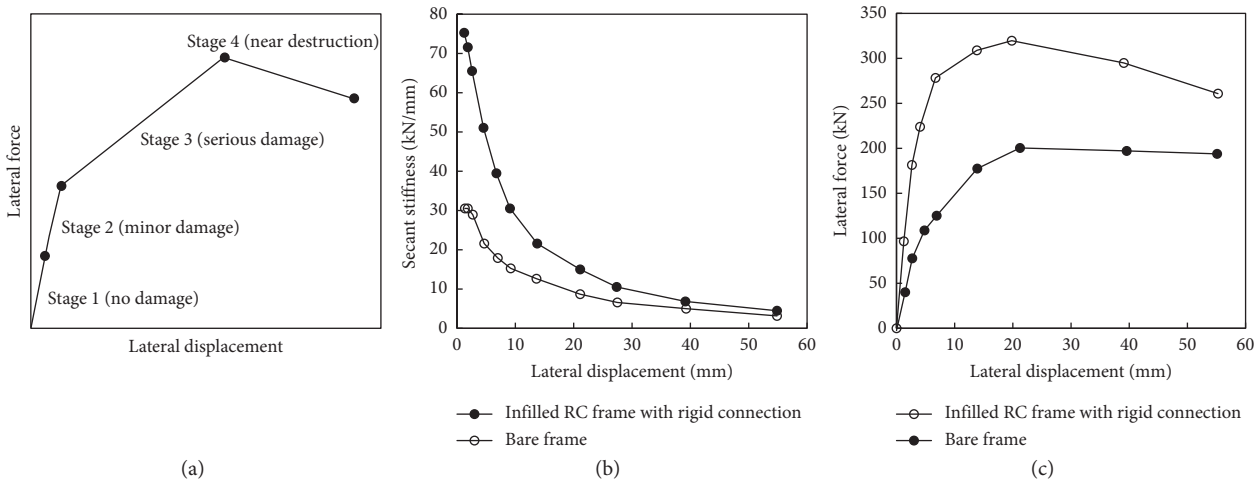

Figure 6: (a) Deformation failure processes; (b) stiffness degradation of two specimens provided by reference [38]; (c) deformation failure processes of two specimens provided by reference [38].

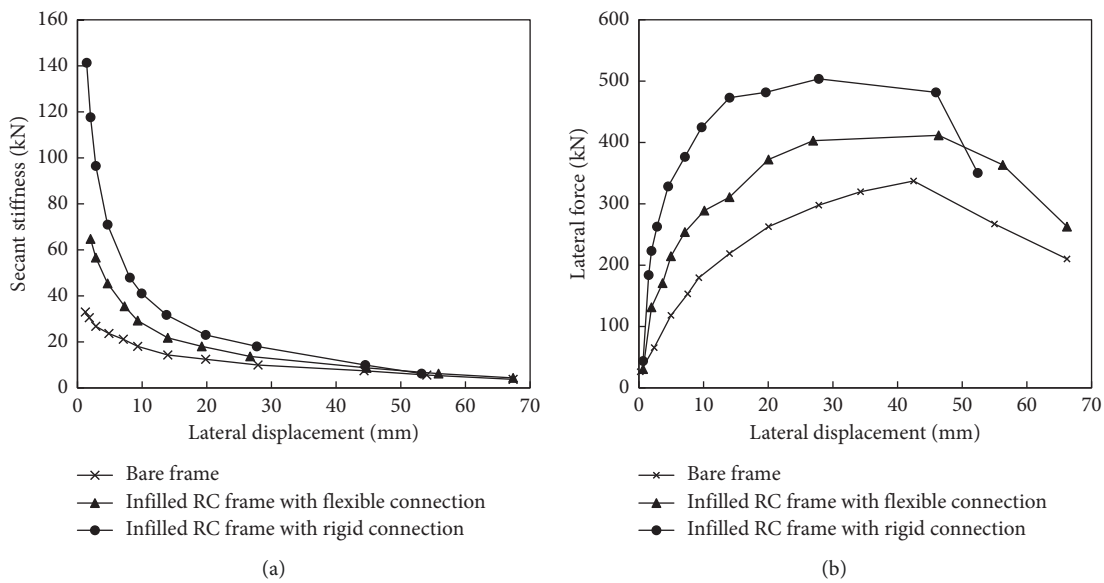

Figure 7: (a) Stiffness degradation of two specimens provided by reference [11]; (b) deformation failure processes of three specimens provided by reference [11].

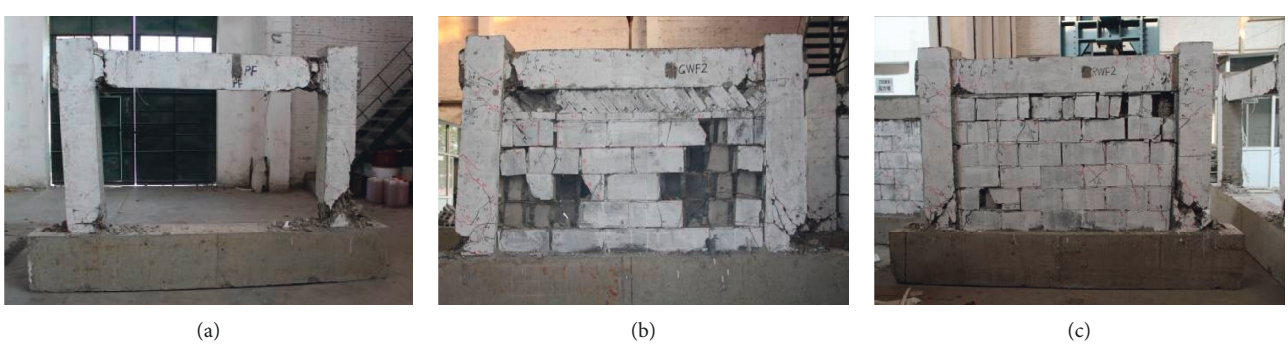

Figure 8: Final failure modes of three specimens provided by reference [11]: (a) bare frame; (b) infilled RC frame with rigid connection; (c) infilled RC frame with flexible connection.

behavior of flexible connection can be accurately simulated. For macrofinite element analysis approach, some simplifications must be adopted.

The effects of flexible connection on lateral stiffness of infilled RC frame are similar to that of opening. So in this study, combined with the macrofinite element simulation methods for infilled RC frame with opening, a simplified analysis method for simulating the effects of flexible connection on infilled RC frame was proposed. The effects of opening on the lateral stiffness of infilled RC frames were deeply investigated by references [33, 34], and the stiffness reduction factor λ, defined as the stiffness of the infill wall with opening to that of the infill wall without opening, was introduced to characterize the effects of opening. According to the research findings provided by references [33, 34], the parameter λ is related to the opening percentage (opening area/infill wall area) and opening position. Figure 10 shows three typical opening positions, named Case A, Case B, and Case C. Figure 11 shows the relationship between stiffness reduction factor and opening percentage (0%~25%) of the above-mentioned cases, and the following findings can be obtained. Firstly, if the opening position is fixed, the increase of opening percentage led to the stiffness degradation of infilled RC frame. Secondly, if the opening percentage is fixed, the opening positions have great influences on the stiffness reduction factor. For above-mentioned cases, the stiffness reduction factor of Case A is the maximum, the second one is Case B, and the stiffness reduction factor of Case C is the minimum. It has been proved that the stiffness reduction factor λ of Case B can be expressed as follows:

$$\lambda = 1 - 2\alpha_{\mathrm{w}}^{0.54} + \alpha_{\mathrm{w}}^{1.14}. \tag{1}$$

In equation (1), α_{w} denotes the opening percentage of infill wall. On this basis, the single-strut model for Case B was proposed by reference [33], and the effectiveness of proposed model was verified through a study case.

For the infilled RC frame with flexible connection, as shown in Figure 1(b), it can be considered as the infilled RC frame with opening, and its location is at the joint area between infill wall and surrounding frame. So in this study, the effects of flexible connection on infilled RC frame are also characterized by stiffness reduction factor λ. According to Section 1, the width of preset crack is in the range of 20 mm~30 mm, so the opening area is much less than the area of infill wall. Therefore, the opening position and opening percentage are approximately fixed, so the stiffness reduction factor λ of flexible connection can be approximately considered as a constant value.

3.2. Model Constructing. Judging from the existing research results, a lot of researchers have studied the macrofinite element numerical simulation methods for infilled RC frame with rigid connection, summarized as single-strut macrofinite element models and multiple-strut macrofinite element models. In this section, based on deeply studying the existing single-strut models for infilled RC frame with rigid connection, an improved single-strut model for infilled RC frame with flexible connection was proposed.

According to references [25, 43, 44], the width (w) of equivalent compressed diagonal strut can be expressed as equations (2)–(4). The above equations were accepted by the majority of researchers dealing with the analysis of infilled RC frame with rigid connection and also recommended by many existing seismic design codes [45–47].

$$\frac{w}{d} = 0.175 \cdot \lambda_h^{-0.4}, \tag{2}$$

$$\lambda_h = \sqrt[4]{\frac{E_{\mathrm{w}} t_{\mathrm{w}} \sin(2\theta)}{4E_{\mathrm{c}} I_{\mathrm{c}} H_{\mathrm{in}}}}, \tag{3}$$

$$\theta = \tan^{-1}\left(\frac{h_{\mathrm{w}}}{L_{\mathrm{w}}}\right). \tag{4}$$

In above equations, d denotes the diagonal length of the infill wall, E_{w} denotes the modulus of elasticity of the infill wall, $E_{\mathrm{c}}I_{\mathrm{c}}$ denotes the flexural rigidity of the columns, t_{w} denotes the thickness of the infill wall and equivalent strut, h denotes the column height between centerlines of beams, L_{w} denotes the length of infill wall, and h_{w} denotes the height of infill wall. The meanings of the above-mentioned parameters are shown in Figure 12.

According to section 3.1, the effect of flexible connection on the lateral stiffness of infilled RC frame is similar to that of opening. Therefore, the stiffness reduction factor λ was introduced to improve equation (2), which can be expressed as follows:

$$\frac{w}{d} = 0.175 \cdot \lambda \cdot \lambda_h^{-0.4}. \tag{5}$$

Therefore, the key problem is to determine the value of stiffness reduction factor (λ). In this study, inversion analysis theory [48, 49] was introduced to solve this problem. Generally speaking, a lot of monitoring instruments are installed in the specimens, such as LVDT, optical fiber, and so on, and during the experimental process, the measured values of effect quantities, such as displacement, force, stress, and so on, will be acquired. The principle of inversion analysis is to make measured values and calculated values as near as possible and, on this basis, seek the optimal values of undetermined parameters. So based on the principle of minimum residual sum of squares, a constrained optimization problem, for estimating the value of stiffness reduction factor, can be constructed:

$$\begin{cases} \min \quad Q(\lambda) = \sum_{i=1}^{n}\sum_{j=1}^{m}\left(\delta_{ij} - \delta'_{ij}\right)^2, \\ \text{s.t.} \quad \underline{\lambda} \le \lambda \le \overline{\lambda}. \end{cases} \tag{6}$$

In equation (6), m denotes the total number of measured values, n denotes the number of monitoring instruments, δ_{ij} denotes the experimental values, δ'_{ij} denotes the calculated value, λ denotes the stiffness reduction factor, $\overline{\lambda}$ denotes the upper limit of parameter λ, and $\underline{\lambda}$ denotes the lower limit of

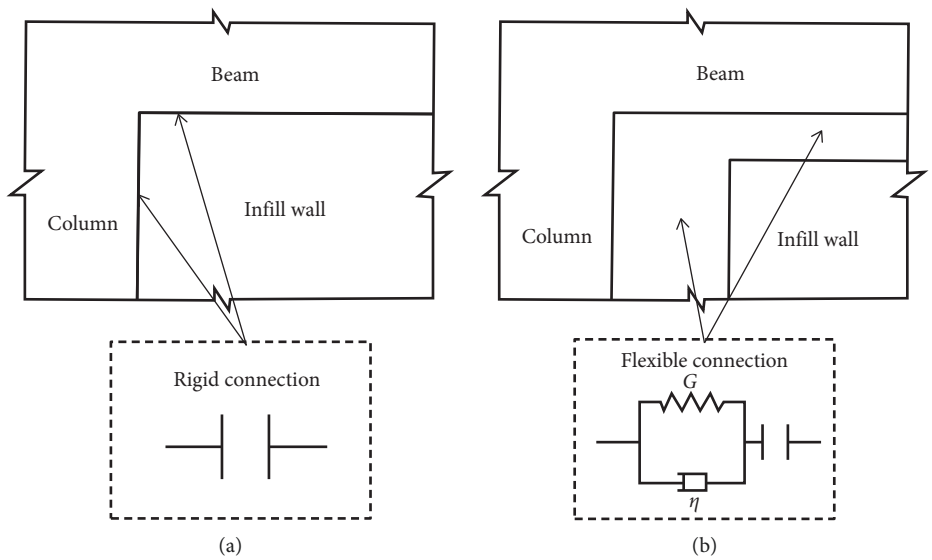

Figure 9: Action patterns of flexible connection and rigid connection.

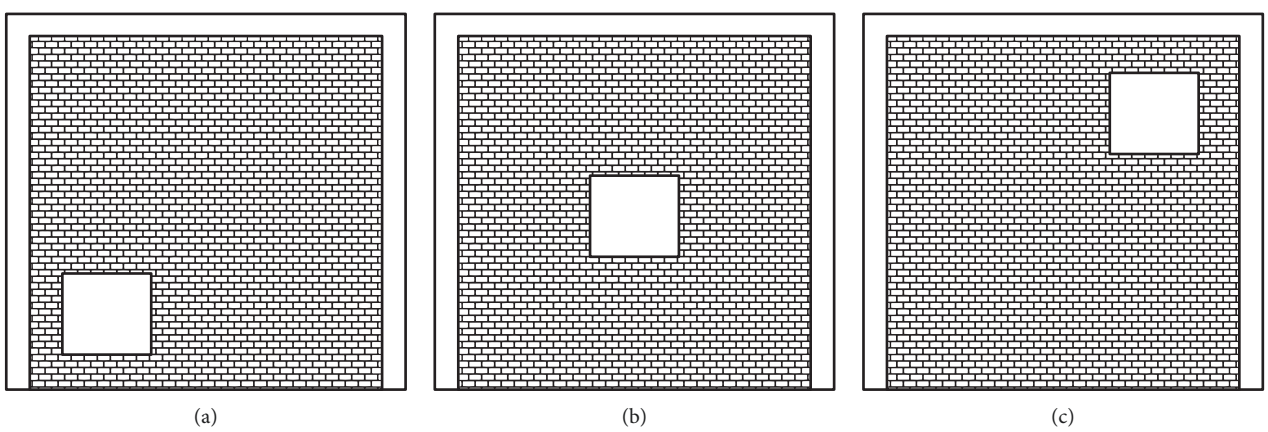

Figure 10: Opening positions. (a) Case A, (b) Case B, (c) Case C.

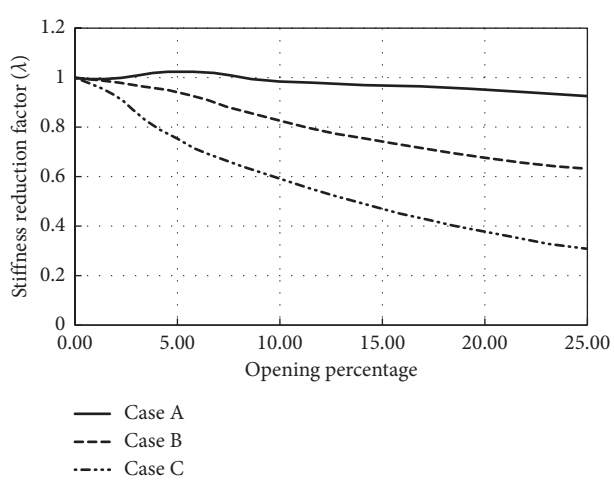

Figure 11: The relationship between the stiffness reduction factor and the opening percentage.

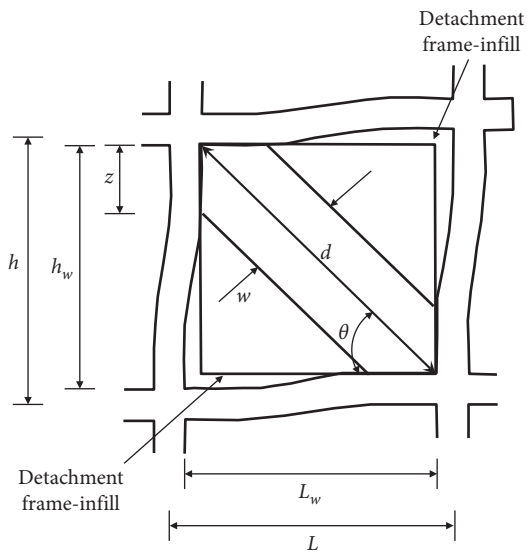

Figure 12: Equivalent diagonal strut model.

parameter λ. Therefore, the estimation problems of parameters in proposed models are transformed into a constrained optimization problem. In this study, the global optimum solution of objective function (6) was searched by artificial fish swarm algorithm (AFSA).

3.3. Parameters Estimation. In nature, a fish moves to the region with more food by vision or sense, and this behavior is called preying. Also, in order to guarantee their existence and avoid danger, nature fish assemble and move in groups, and this behavior is called swarming. What's more, if a fish researches a region with more food, the other fish will trail and reach this region, and this behavior is called chasing. On the basis of above-mentioned behaviors, artificial fish swarm algorithm (AFSA) [50–52] possesses a high search speed and global search capability.

If a minimization problem having D-dimensional search space, N denotes the population quantity of artificial fish swarm. $X_i = (x_{i1}, x_{i2}, \ldots, x_{iD})$ denotes the position of artificial fish i. The food concentration at position X_i is denoted by $Q(X_i)$. The distance between X_i and X_j is denoted by $d_{ij} = X_i - X_j$. The parameter *Step* denotes the largest allowed space step of an artificial fish. δ denotes the crowded degree of artificial fish swarm. *Visual* denotes the visible range of an artificial fish. t denotes the iteration number. *Num* denotes the maximum number of iterations. If the number of iterations is greater than *Num*, the iteration will be suspended; otherwise, continue iterating.

The preying behavior of artificial fish swarm has been described below. Suppose the initial state of artificial fish i is denoted by X_i, this artificial fish randomly chooses a new state within its visual, and the new state X_i' can be expressed as follows [50]:

$$X_i' = X_i + \text{rand}(0,1) \times \text{visual}. \tag{7}$$

If $f(X_j) < f(X_i')$, the artificial fish i moves toward to $X_i^{(t+1)}$, based on the equations (8) and (9) [51, 52]:

$$X_i^{(t+1)} = X_i^{(t)} + \text{rand}(0.1) \times \text{step} \times \frac{X_j^{(t)} - X_i^{(t)}}{\left\|\mathbf{X}_j^{(t)} - \mathbf{X}_i^{(t)}\right\|}, \tag{8}$$

$$\left\|\mathbf{X}_j^{(t)} - \mathbf{X}_i^{(t)}\right\| = \left|\sqrt{\left(X_j^{(t)}\right)^2 - \left(X_i^{(t)}\right)^2}\right|. \tag{9}$$

If $f(X_j) > f(X_i')$, the artificial fish i selects another state randomly. If the artificial fish i fails to find a feasible solution within the given time, under this circumstance, it moves one step randomly, based on equation (10) [53, 54]:

$$X_i^{(t+1)} = X_i^{(t)} + \text{rand}(0,1) \times \text{step}. \tag{10}$$

The swarming behavior of artificial fish swarm has been described below. Suppose the present position of an artificial fish is denoted by X_i, *nf* denotes the number of artificial fish within a particular visual, X_c denotes the center position of artificial fish swarm, and Y_c denotes the food concentration of X_c. X_c and Y_c can be expressed as follows:

$$X_c = \sum_j^{nf} \frac{X_j}{nf}, \qquad Y_c = Q(X_c). \tag{11}$$

If $(Y_c/nf) < \delta Y_i$, then this is not a crowed area. Otherwise, the artificial fish i moves toward $X_i^{(t+1)}$ in the following direction [55]:

$$X_i^{(t+1)} = X_i^{(t)} + \text{rand}(0.1) \times \text{Step} \times \frac{X_c^{(t)} - X_i^{(t)}}{\left\|\mathbf{X}_j^{(t)} - \mathbf{X}_i^{(t)}\right\|}. \tag{12}$$

If swarming is not advantageous, AFSA executes the preying behavior.

The chasing behavior of artificial fish swarm was described below. Suppose the present position of an artificial fish is denoted by X_i, X_m denotes the best position with highest food consistence within artificial fish i's visual, and *nf* denotes the number of artificial fish within a particular visual. If $(Y_m/nf) > \delta Y_i$, the artificial fish i moves one step toward $X_i^{(t+1)}$, which can be expressed as follows [54, 56]:

$$X_i^{(t+1)} = X_i^{(t)} + \text{rand}(0.1) \times \text{step} \times \frac{X_m^{(t)} - X_i^{(t)}}{\left\|\mathbf{X}_j^{(t)} - \mathbf{X}_i^{(t)}\right\|}, \tag{13}$$

If this is not advantageous, AFSA also executes the preying behavior.

4. Simulation and Analysis

The Open System for Earthquake Engineering Simulation (OpenSEES) is a software framework for simulating the seismic response of structural and geotechnical systems. It provides a wide range of element types and material models for nonlinear finite element analysis [56–59]. According to the quasistatic experiment performed by Zhou et al. [11, 24], three specimens were tested under the action of horizontal lateral cyclic force, one specimen is a bare frame (PF), one is an infilled RC frame with rigid connection (GWF1), and

another one is an infilled RC frame with flexible connection (RWF1). In this section, based on the experiment results provided by references [11, 24], OpenSEES was applied to the numerical simulation analysis, and then a case study was conducted to verify the effectiveness and feasibility of proposed model.

4.1. Modeling Details. The dimensions and reinforcements of beams and columns are shown in Figure 13. The lateral loading protocol is shown in Figure 14. In the computational model, beams and columns were represented by displacement-based beam-column element, and cross sections were defined using fiber discretization with distinct layers for longitudinal reinforcement [60]. Equivalent diagonal struts were represented by truss element.

For material model used in this paper, the longitudinal steel bar was modeled by Steel01 (Figure 15(a)), masonry was modeled by Concrete01 (Figure 15(b)), and concrete was modeled by Concrete02 (Figure 15(c)). The material parameters of concrete, rebar, and masonry are shown in Tables 1–3, respectively. Confining effect due to the prescribed transverse reinforcement is accounted for using confined concrete properties for core concrete material as suggested by Mander et al. [61, 62].

The model proposed by Zhao and Sritharan [63] was used to characterize the stress and end slip response of steel rebar. This model imitates the strain penetration effects using the zero-length section element [60]. A zero-length section element includes one section corresponding to one integration point, which determines the force-deformation response of the element. The function embodied in Figure 16 depicts the envelope of the bar stress versus the slip response at the end of the flexural member. The slip at the point that the bar stress reaches the yield (s_y) and ultimate strengths (s_u) are obtained from the equations (14) and (15), respectively:

$$s_y = 0.1\left[\frac{d_b}{4}\frac{f_y}{\sqrt{f'_c}}(2\alpha+1)\right]^{1/\alpha} + 0.0134, \tag{14}$$

$$s_u = 35 s_y. \tag{15}$$

In equations (14) and (15), d_b (in) denotes the diameter of rebar, f_y (ksi) and f'_c(ksi) denote the yield strength of rebar and compressive strength of concrete, respectively, and the parameter α is set to 0.4.

4.2. Simulation Results of PF and GWF1. In this section, nonlinear pushover analysis and nonlinear hysteretic analysis for PF and GWF1 were conducted, respectively. Based on the equations (2)–(4), the parameters of equivalent diagonal strut model for GWF1 can be determined, as listed in Table 4. Figure 17 shows the comparison between nonlinear pushover analysis results and corresponding experiment results of PF and GWF1. According to the calculation results, in the stage of linear deformation, the simulation results approach to the measured values. Due to measurement errors, limitations of material models, and so on, there exist some deviations between the simulation results and the experiment results in the stage of nonlinear deformation. However, these deviations are permissible in engineering practice. The comparison between nonlinear hysteretic analysis result and corresponding experiment result of for GWF1 is shown in Figure 18(a), and the comparison between simulation result and experiment result of stiffness degradation of GWF1 during the process of pushover is shown in Figure 18(b). According to the calculation results, the equivalent diagonal strut model for infilled RC frame with rigid connection is effective and can reflect the characteristics of wall-frame interaction.

4.3. Simulation Results of RWF1. According to the lateral loading protocol as shown in Figure 14, the objective function (6) can be written as follows:

$$\begin{cases} \min \quad Q(\lambda) = \sum_{j=1}^{m}\left(F_j - F'_j\right)^2, \\ \text{s.t.} \quad \underline{\lambda} \le \lambda \le \overline{\lambda}. \end{cases} \tag{16}$$

In equation (16), F_i denotes the measured value of lateral force at the control displacement i, F'_i denotes the calculated value of lateral force at the control displacement i, λ denotes the stiffness reduction factor, $\overline{\lambda}$ denotes the upper limit of parameter λ, and $\underline{\lambda}$ denotes the lower limit of parameter λ. Figure 19 shows the comparison between pushover analysis results and corresponding experiment results under different stiffness reduction conditions. According to the calculation results, the decrease of stiffness reduction factor leads to the decrease of initial lateral stiffness and bearing capacity of FEM model for RWF1. Moreover, due to measurement errors, limitations of material models, and so on, there exist some deviations between the simulation results and experiment results in the nonlinear stage. Therefore, based on the principle of inversion analysis introduced in Section 3.2, the experiment values of linear stage were applied to determine the stiffness reduction factor of flexible connection.

Generally speaking, the stiffness reduction factor λ is in the range of [0, 1]. The parameters of AFSA were listed as follows: N was set to 20, *Visual* was set to 1, δ was set to 0.618, *Step* was set to 0.5, *Num* was set to 200, and the convergence threshold ε was set to 1×10^{-4}. The optimization process of AFSA is shown in Figure 20. According to the optimization results, AFSA converged with 70 iterations, and the convergence value of stiffness reduction factor was equal to 0.52. Therefore, the strut width w of improved equivalent diagonal strut for infilled RC frame with flexible connection can be expressed as follows:

$$w = 0.091 \cdot \lambda_h^{-0.4} \cdot d, \tag{17}$$

$$\lambda_h = \sqrt[4]{\frac{E_w t_w \sin(2\theta)}{4E_c I_c H_{in}}}. \tag{18}$$

Employed with the equations (17) and (18), the parameters of the equivalent diagonal strut model for RWF1 are

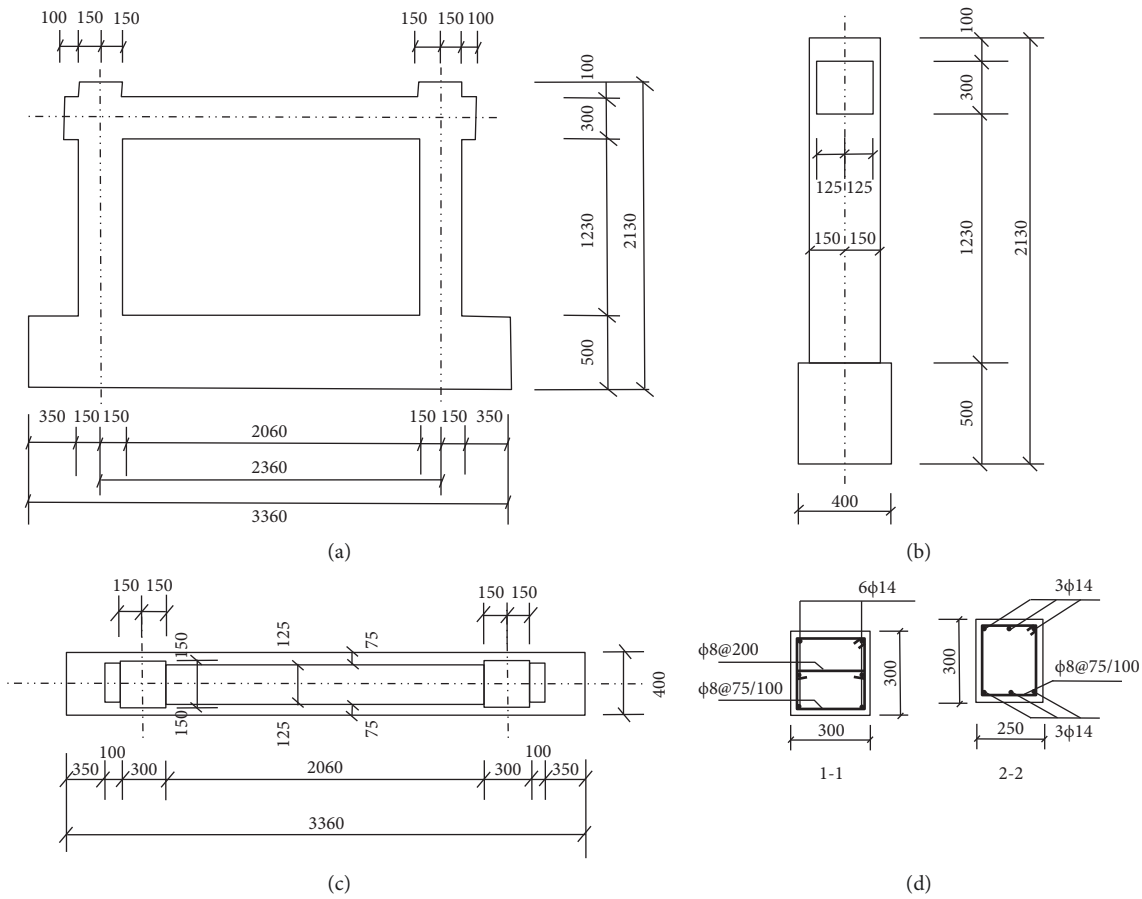

Figure 13: Dimensions and reinforcements of RC frame.

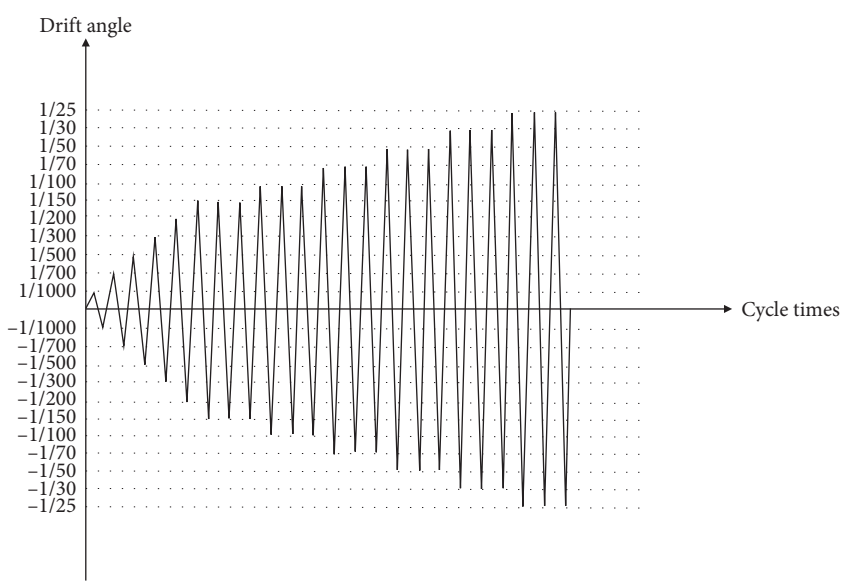

Figure 14: Lateral loading protocol.

shown in Table 5. The comparison between nonlinear hysteretic analysis result and corresponding experiment result is shown in Figure 21(a), and the comparison between simulation result and experiment result of stiffness degradation of GWF1 during the process of pushover is shown in Figure 21(b). According to the calculation results, the model proposed in this study can reflect the in-plane behavior of infilled RC frame with flexible connection effectively.

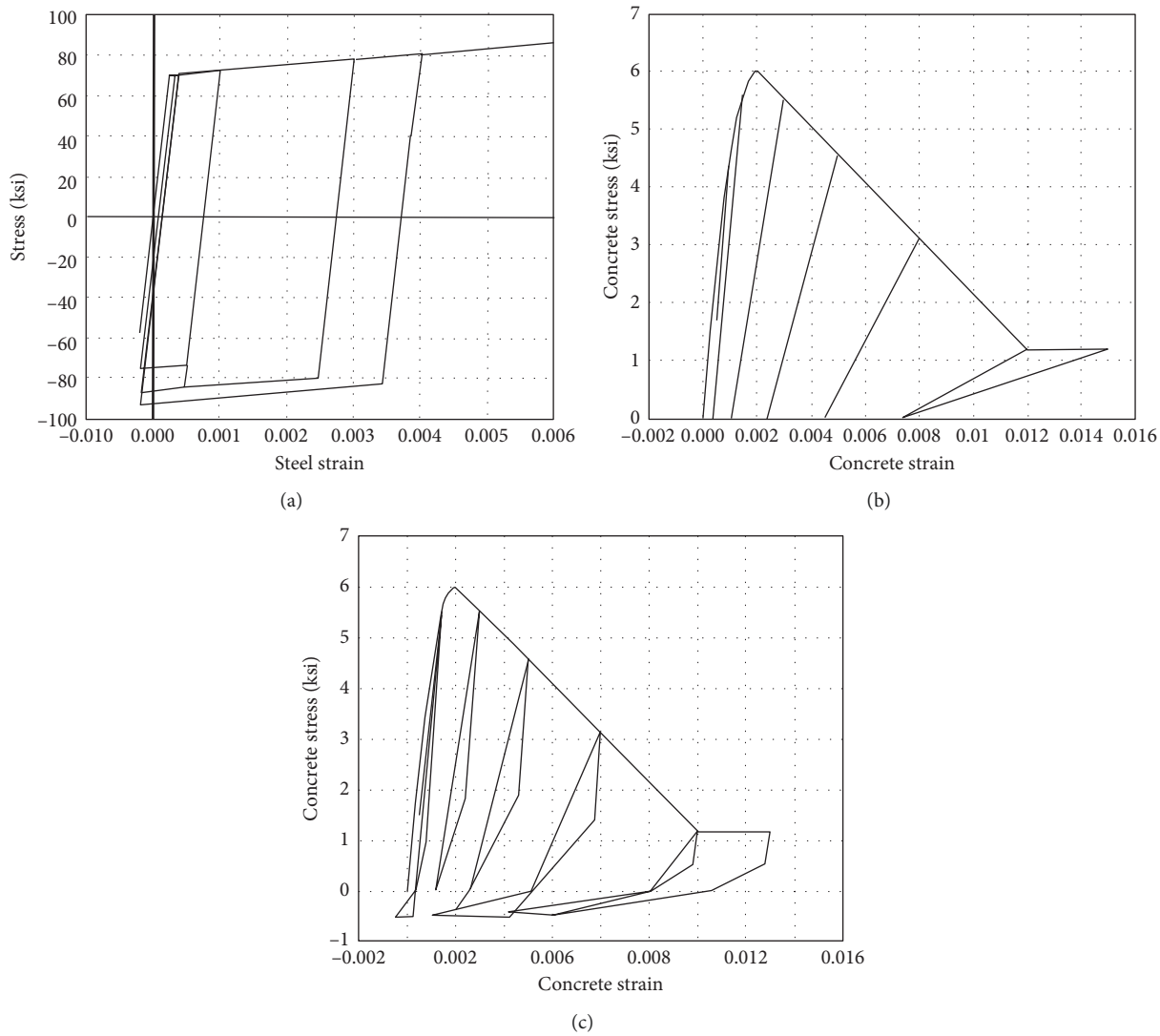

Figure 15: Material models [60].

Table 1: Parameters of concrete material [24].

Parameters	Beams	Columns
Concrete compressive strength (MPa)	23.6	25.6
Concrete strain at maximum strength	0.0035	0.00447
Concrete crushing strength (MPa)	20.06	21.76
Concrete strain at crushing strength	0.0129	0.018
Ratio between unloading slope (ultimate compression strain) and initial slope	0.5	0.5
Tensile strength (MPa)	2.26	2.26
Tension softening stiffness (MPa)	2.26×10^3	2.26×10^3

Table 2: Parameters of steel material [24].

Parameters	Beams	Columns
Initial modulus of elasticity (MPa)	2×10^5	2×10^5
Yield strength (MPa)	483.8	483.8
Strain-hardening ratio	0.01	0.01

Table 3: Parameters of masonry material [24].

Parameters	Columns
Concrete compressive strength (MPa)	1.02
Concrete strain at maximum strength	0.0023
Concrete crushing strength (MPa)	0.5377
Concrete strain at crushing strength	0.0046

5. Conclusion

During the 2008 Wenchuan earthquake, a lot of masonry-infilled RC frame structures suffered serious damages due to the detrimental effects brought about by infill wall rigidly connected to surrounding frame. In order to solve this problem, the flexible connection, introduced by Chinese designers, is recommended by the updated Chinese seismic design code. Although infilled RC frame structure with flexible connection has a lot of advantages, but because of the lack of research, this structure type is seldom used in practical engineering. Therefore, it is of great significance to scientifically analyze and investigate the effects of flexible connection on structure behaviors of infilled RC frame. So in this study,

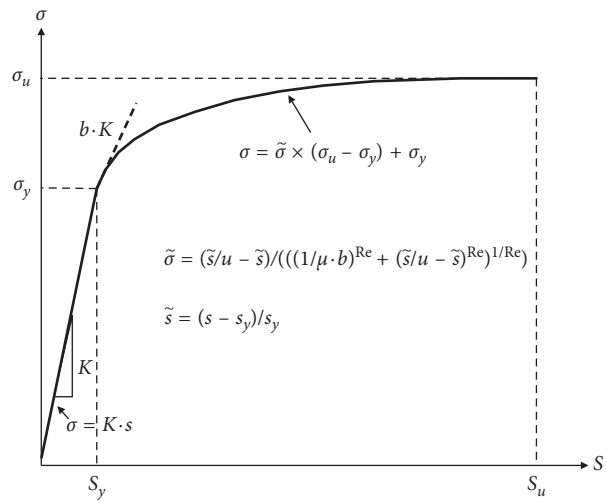

Figure 16: Steel bar stress versus slip for completely anchored reinforcing bars into footings.

Table 4: Parameters of equivalent diagonal strut model for GWF1.

E_w (MPa)	E_c (MPa)	a (mm)	b (mm)	I_c (mm^4)	t_w (mm)	$\sin\theta$
443	5727.07	300	300	6.75×10^8	240	0.513
$\cos\theta$	d (mm)	h (mm)	l_b	H_{in} (mm)	λ_h	w (mm)
0.859	2399.27	1380	2360	1230	0.00149	533.439

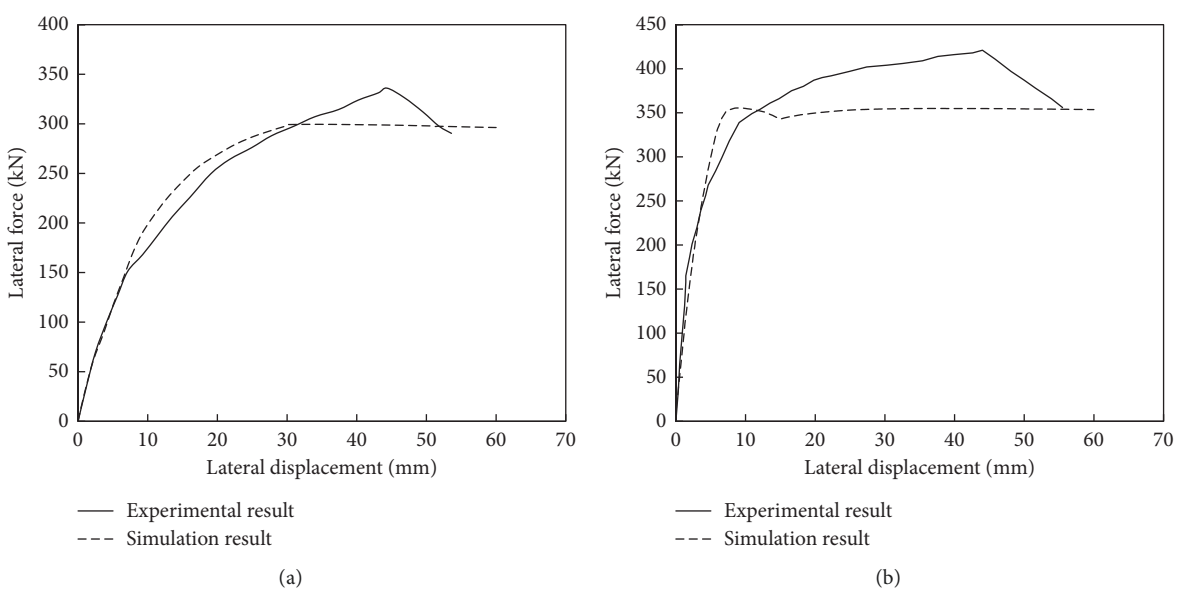

Figure 17: Comparison between pushover analysis results and experiment results: (a) PF; (b) GWF1.

an improved equivalent diagonal strut model for masonry-infilled RC frame with flexible connection was developed. Accordingly, the following conclusions are drawn:

(1) Based on deeply studying and analyzing the existing research achievements, the effects of connection on in-plane behaviors of infilled RC frame were discussed. Although the effects of flexible connection on initial lateral stiffness and bearing capacity of frame structure are inferior to that of rigid connection, it can reduce the unfavorable interaction between infill wall and surrounding frame, retard the stiffness degradation, and effectively improve the seismic performance of frame structure. Especially for the effect of flexible connection on the initial lateral stiffness of infilled RC frame, its effects are similar to that of opening.

(2) Based on discussing the action pattern of flexible connection and applied with the macrofinite element

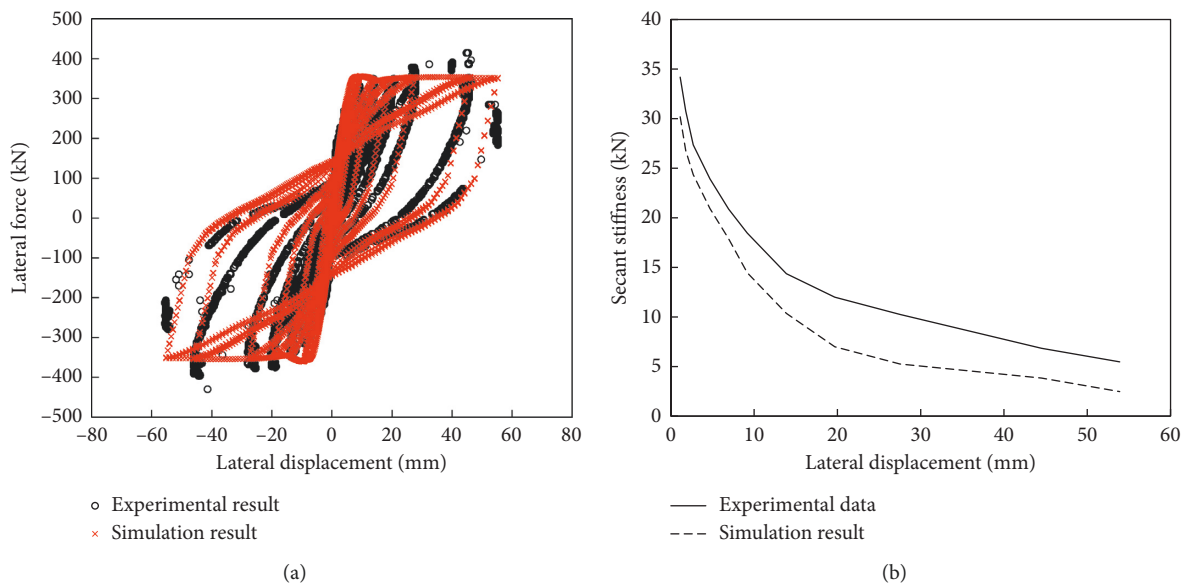

Figure 18: Comparison between simulation results and experiment results of GWF1: (a) hysteresis loop; (b) stiffness degradation.

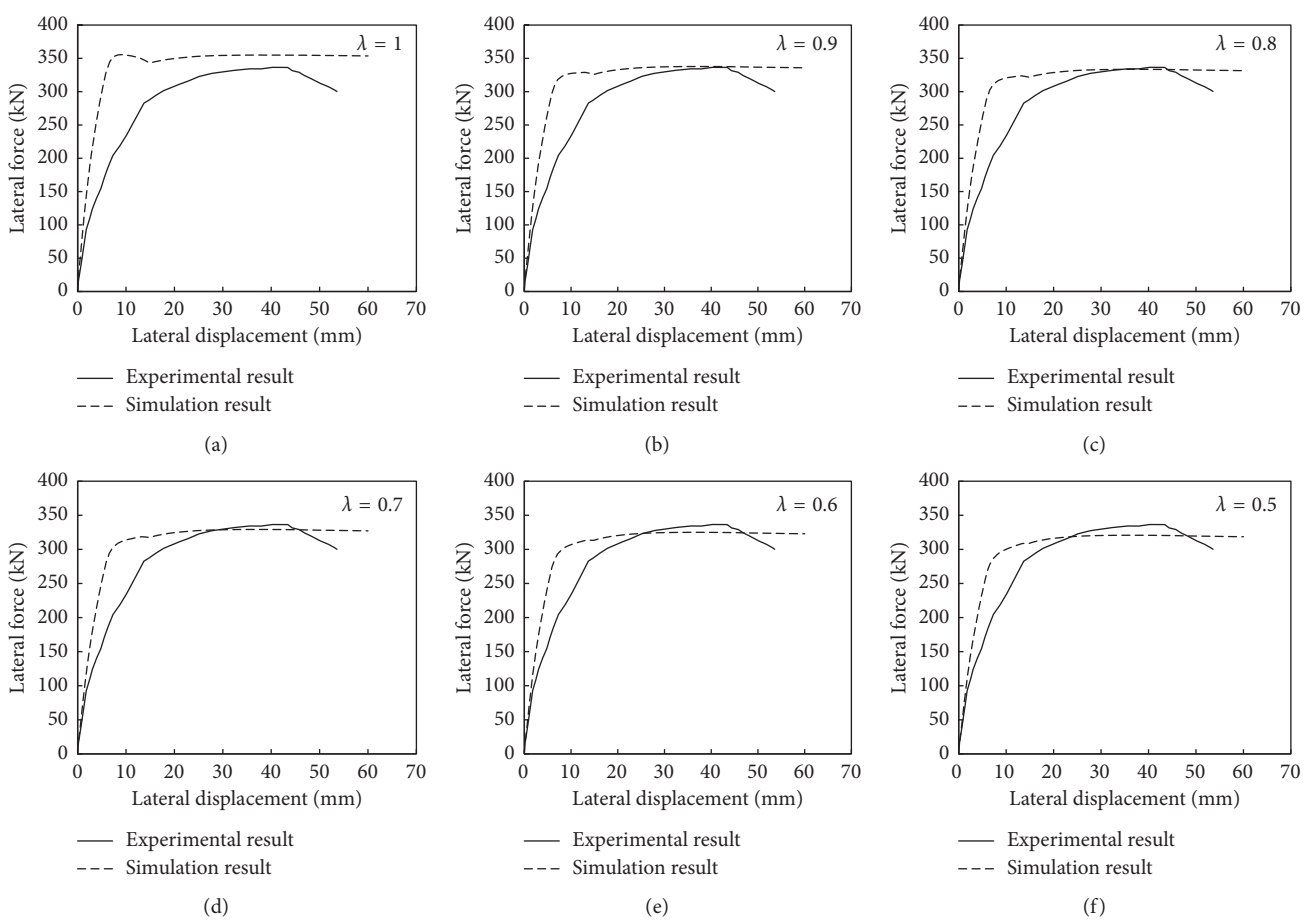

Figure 19: Continued.

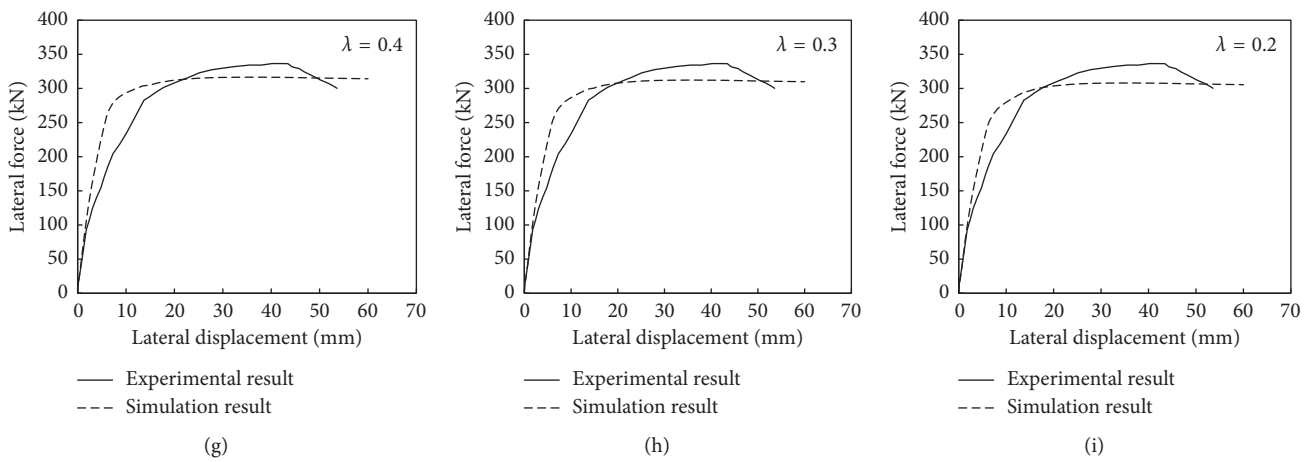

Figure 19: Comparison between pushover analysis results and experiment results under different stiffness reduction conditions.

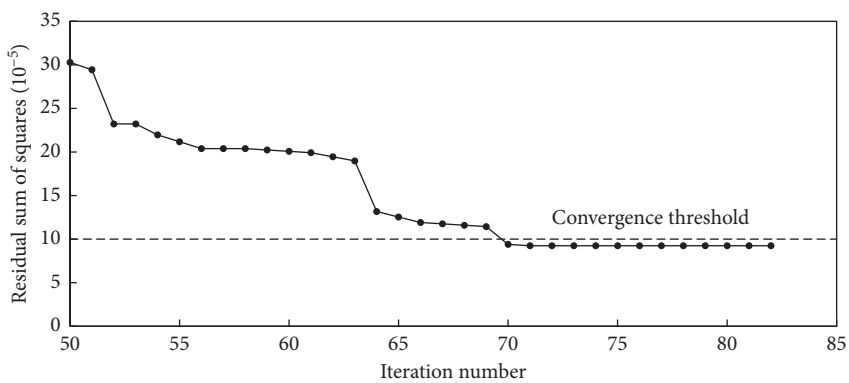

Figure 20: Optimization process of AFSA.

Table 5: Parameters of improved equivalent diagonal strut model for RWF1.

E_w (MPa)	E_c (MPa)	a (mm)	b (mm)	I_c (mm^4)	t_w (mm)	$\sin\theta$
443	5727.07	300	300	6.75×10^8	240	0.513
$\cos\theta$	d (mm)	h (mm)	l_b	H_{in} (mm)	λ_h	w (mm)
0.859	2399.27	1380	2360	1230	0.00149	277.388

simulation methods for infilled RC frame with opening, the stiffness reduction factor λ was introduced to characterize the effects of flexible connection on lateral stiffness of infilled RC frame. Moreover, on the basis of analyzing the structure characteristics of infilled RC frame with flexible connection, the conclusion that the stiffness reduction factor of flexible connection is approximately a constant value was drawn. Then, combined with the existing equivalent diagonal strut models for infilled RC frames with rigid connection, an improved equivalent diagonal strut model for infilled RC frame with flexible connection was proposed.

(3) Inversion theory was introduced to determine the value of stiffness reduction factor, and the principle is to make measured values and calculated values as near as possible. Based on minimum residual sum of squares, a constrained optimization problem, for estimating stiffness reduction factor, was constructed, and then artificial fish swarm algorithm (AFSA) was applied to search the global optimum solution of objective function through preying behavior, swarming behavior, and chasing behavior.

(4) Up to now, relevant experimental and numerical researches about infilled RC frame with flexible connection are very less and need to be further urgently. In this study, only applied with the experiment results provided by reference [11, 24], the stiffness reduction factor λ was determined through AFSA, and on this basis, an improved equivalent diagonal strut model for infilled RC frame with flexible connection was proposed. Therefore, the effectiveness and feasibility of the proposed model need to be further verified based on more experiment results. Moreover,

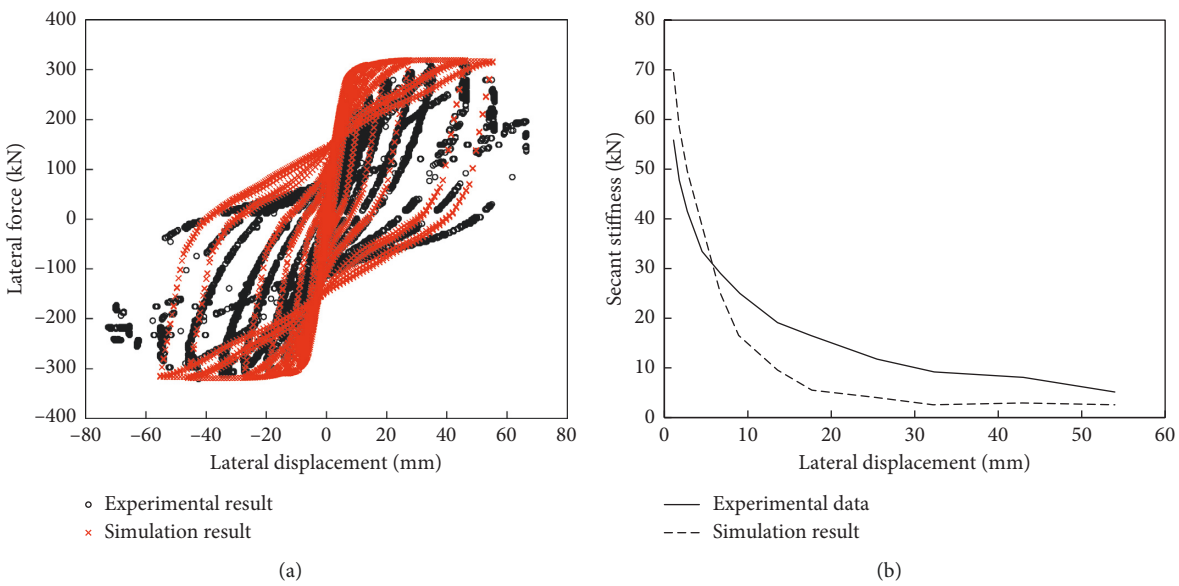

Figure 21: The result of hysteretic analysis and nonlinear pushover analysis (RWF1).

it is worthwhile pointing out that the analysis method based on inversion theory can be extended to build more accurate models for infilled RC frame with flexible connection, such as multiple-struts models.

Data Availability

The data used to support the findings of this study are available from the corresponding author upon request.

Conflicts of Interest

The authors declare no conflicts of interest.

Authors' Contributions

Y. G. conceptualized the study; Y. G. and L. X. Y. performed data curation; Y. G. and Z. E. F. supervised the study; Y. G., L. X. Y., Z. E. F., E. N. T., K. K., and Z. W. performed formal analysis; Y. G. and L. X. Y. wrote the original draft; Y. G., Z. E. F., L. X. Y, E. N. T., K. K., and Z. W reviewed and edited the article.

Acknowledgments

This study was supported by the Central University Basic Research Project (grant no. 2017B40214), National Key R&D Program of China (2016YFC0401601 and 2017YFC0804607), National Natural Science Foundation of China (grant nos. 51739003, 51479054, 51779086, 51579086, 51379068, 51579083, 51579085, and 51609074), Project Funded by the Priority Academic Program Development of Jiangsu Higher Education Institutions (YS11001), Jiangsu Natural Science Foundation (grant no. BK20160872), Special Project Funded of National Key Laboratory (20145027612 and 20165042112), and Key R&D Program of Guangxi (AB17195074).

References

[1] China Architecture and Building Press, *Technical specification for concrete small-sized hollow block masonry buildings (JGJ/T 14-2011)*, China Architecture and Building Press, Bejing, China, 2011, in Chinese.

[2] Z. F. Yuan, L. Yuan, and B. Liu, "Discussion on design and application of masonry filled walls separated from frame columns," *Building Structure*, vol. 40, no. 5, pp. 112–116, 2010, in Chinese.

[3] F. G. Thomas, "The strength of brickwork," *Journal of Structural Engineering*, vol. 31, pp. 35–46, 1953.

[4] A. B. Mehrabi, P. Benson Shing, M. P. Schuller, and J. L. Noland, "Experimental evaluation of masonry-infilled RC frames," *Journal of Structural Engineering*, vol. 122, no. 3, pp. 228–237, 1996.

[5] K. C. Stylianidis, "Experimental investigation of masonry infilled RC frames," *Open Construction and Building Technology Journal*, vol. 6, no. 1, pp. 194–212, 2012.

[6] D. J. Kakaletsis and C. G. Karayannis, "Influence of masonry strength and openings on infilled R/C frames under cycling loading," *Journal of Earthquake Engineering*, vol. 12, no. 2, pp. 197–221, 2008.

[7] L. Cavaleri and F. Di Trapani, "Cyclic response of masonry infilled RC frames: experimental results and simplified modeling," *Soil Dynamics and Earthquake Engineering*, vol. 65, pp. 224–242, 2014.

[8] D. J. Kakaletsis and C. G. Karayannis, "Experimental investigation of infilled reinforced concrete frames with openings," *ACI Structural Journal*, vol. 106, no. 2, pp. 132–41, 2009.

[9] D. Mallick and R. Garg, "Effect of openings on the lateral stiffness of infilled frames," *Proceedings of the Institution of Civil Engineers*, vol. 49, no. 2, pp. 193–209, 1971.

[10] H. Jiang, X. Liu, and J. Mao, "Full-scale experimental study on masonry infilled RC moment-resisting frames under cyclic loads," *Engineering Structures*, vol. 91, pp. 70–84, 2015.

[11] X. J. Zhou, X. L. Jiang, D. D. Xu, J. K. Song, and C. H. Yang, "Experimental research on seismic behavior of flexible

connection frame structure infilled with new masonry," *Word earthquake engineering*, vol. 31, no. 1, pp. 58–67, 2015, in Chinese.

[12] Q. Peng, X. Zhou, and C. Yang, "Influence of connection and constructional details on masonry-infilled RC frames under cyclic loading," *Soil Dynamics and Earthquake Engineering*, vol. 108, pp. 96–110, 2018.

[13] H. R. Lotfi, *Finite element analysis of fracture of concrete and masonry structures*, Ph.D. Thesis, University of Colorado Boulder, Boulder, Colorado, 1992.

[14] P. B. Lourenco, *Computational strategies for masonry structures*, Ph.D. Thesis, Delft University of Technology, Delft, Netherlands, 1996.

[15] A. B. Mehrabi and P. B. Shing, "Finite element modeling of masonry-infilled RC frames," *Journal of Structural Engineering*, vol. 123, no. 5, pp. 604–613, 1997.

[16] Y.-J. Chiou, J.-C. Tzeng, and Y.-W. Liou, "Experimental and analytical study of masonry infilled frames," *Journal of Structural Engineering*, vol. 125, no. 10, pp. 1109–1117, 1999.

[17] M. M. Attard, A. Nappi, and F. Tin-Loi, "Modeling fracture in masonry," *Journal of Structural Engineering*, vol. 133, no. 10, pp. 1385–1392, 2007.

[18] G. Al-Chaar, A. B. Mehrabi, and T. Manzouri, "Finite element interface modeling and experimental verification of masonry-infilled R/C frames," *Masonry Society Journal*, vol. 26, no. 1, pp. 47–65, 2008.

[19] A. Stavridis and P. B. Shing, "Finite-element modeling of nonlinear behavior of masonry-infilled RC frames," *Journal of Structural Engineering*, vol. 136, no. 3, pp. 285–296, 2010.

[20] D. Mallick and R. Seven, "Dynamic characteristics of infilled frames," *Proceedings of the Institution of Civil Engineers*, vol. 39, no. 2, pp. 261–287, 1968.

[21] P. B. Lourenço, "Computations on historic masonry structures," *Progress in Structural Engineering and Materials*, vol. 4, no. 3, pp. 301–319, 2002.

[22] D. M. Cotsovos, N. D. Stathopoulos, and C. A. Zeris, "Behavior of RC beams subjected to high rates of concentrated loading," *Journal of Structural Engineering*, vol. 134, no. 12, pp. 1839–1851, 2008.

[23] W. J. Wu, "*Study on the seismic performance of the infilled RC frames with openings*," M.S. Thesis, Chang'an University, Xi'an, China, 2018.

[24] X. J. Zhou, P. Q. Chen, and Y. L. Wang, "Finite element calculation and experiment comparison about masonry-infilled frame structure considering and connection ways between infill wall and frame," *Word Earthquake Engineering*, vol. 31, no. 2, pp. 188–195, 2015, in Chinese.

[25] M. Holmes, "Steel frames with brickwork and concrete infilling," *Proceedings of the Institution of Civil Engineers*, vol. 19, no. 4, pp. 473–478, 1961.

[26] J. L. Dawe and C. K. Seah, "Analysis of concrete masonry infilled steel frames subjected to in-plane loads," in *Proceedings of the 5th Canadian Masonry Symposium*, pp. 329–340, Vancouver, BC, Canada, June 1989.

[27] A. J. Durrani and Y. H. Luo, "Seismic retrofitofflat-slab buildings with masonry infill," in *Proceedings of the NCEER Workshop on Seismic Response of Masonry Infills, Report NCEER-94-0004*, San Francisco, CA, USA, February 1994.

[28] R. J. Mainstone, "On the stiffness and strength of infilled frames," *Proceedings of Institute of Civil Engineers*, vol. 7360S, pp. 57–89, 1971.

[29] F. J. Crisafulli, *Seismic Behaviour of Reinforced Concrete Structures with Masonry Infills*, University of Canterbury, Christchurch, New Zealand, 1997.

[30] F. J. Crisafulli and A. J. Carr, "Proposed macro-model for the analysis of infilled frame structures," *Bulletin of the New Zealand Society of Earthquake Engineering*, vol. 40, pp. 69–77, 2007.

[31] C. Z. Chrysostomou, P. Gergely, and J. F. Abel, "A six-strut model for nonlinear dynamic analysis of steel infilled frames," *International Journal of Structural Stability and Dynamics*, vol. 2, pp. 335–353, 2003.

[32] W. W. El-Dakhakhni, M. Elgaaly, and A. A. Hamid, "Three-strut model for concrete masonry-infilled steel frames," *Journal of Structural Engineering*, vol. 129, no. 2, pp. 177–185, 2003.

[33] J. C. Kong, *Seismic performance of masonry infilled rc frame structures with openings*, Ph.D. Thesis, Harbin Institute of Technology, Harbin, China, 2017, in Chinese.

[34] A. Giannakas, D. Patronis, and M. Fardis, "The influence of the position and the size of openings to the elastic rigidity of infill walls," *Proc. 8th Hellenic Concrete Conf.*, pp. 49–56, 1987.

[35] H. Mostafaei and T. Kabeyasawa, "Effect of infill masonry walls on the seismic response of reinforced concrete buildings subjected to the 2003 Bam earthquake strong motion: a case study of Bam telephone center," *Bulletin of the Earthquake Research Institute*, vol. 79, pp. 133–156, 2004.

[36] Q. Q. Zhang, "*Study on earthquake resistance behavior impact of infill walls on reinforced concrete frame structure*," M.S. Thesis, Harbin Institute of Technology, Harbin, China, 2013, in Chinese.

[37] L. Cavaleri, F. Di Trapani, P. G. Asteris, and V. Sarhosis, "Influence of column shear failure on pushover based assessment of masonry infilled reinforced concrete framed structures: a case study," *Soil Dynamics and Earthquake Engineering*, vol. 100, pp. 98–112, 2017.

[38] Q. X. Huang, *Study on seismic behavior and elastic-plastic analysis method for seismic responses of RC frame infilled with new masonry*, Ph.D. Thesis, Huaqiao University, Xiamen, China, 2011, in Chinese.

[39] S. Gómez-Fernández, M. Günther, B. Schartel, M. A. Corcuera, and A. Eceiza, "Impact of the combined use of layered double hydroxides, lignin and phosphorous polyol on the fire behavior of flexible polyurethane foams," *Industrial Crops and Products*, vol. 125, pp. 346–359, 2018.

[40] X. Wang, S. He, G. Wang et al., "Characterization of PBDD/F emissions from simulated polystyrene insulation foam via lab-scale programmed thermal treatment testing," *Chemosphere*, vol. 211, pp. 926–933, 2018.

[41] C. Li, G. Chen, W. Wang et al., "Grain boundary passivation by CdCl2 treatment in CdTe solar cells revealed by Kelvin probe force microscopy," *Journal of Materials Science: Materials in Electronics*, vol. 29, no. 24, pp. 20718–20725, 2018.

[42] H. G. Jin, H. J. Li, and G. G. Sun, "Analysis of interaction between reinforced concrete frame and infilled wall subject to earthquake-induced ground motion," *Earthquake Engineering And Engineering Dynamics*, vol. 37, no. 4, pp. 31–41, 2017, in Chinese.

[43] B. S. Smith, "Behavior of square inflled frames," *American Society of Civil Engineers*, vol. 92, no. 1, pp. 381–403, 1966.

[44] B. S. Smith and C. Carter, "A method of analysis for inflled frames," *Proceedings of the Institution of Civil Engineers*, vol. 44, pp. 31–48, 1969.

[45] R. J. Mainstone and G. A. Weeks, "The influence of a bounding frame on the racking stiffness and strength of brick walls," in *Proceedings of the 2nd International Brick Masonry Conference*, pp. 165–171, Stoke-on-Trent, UK, April 1970.

[46] FEMA-274, *NEHRP Commentary on the Guidelines for the Seismic Rehabilitation of Buildings*, Federal Emergency Management Agency, Washington DC, USA, 1997.

[47] FEMA-306, *Evaluation of Earthquake Damaged Concrete and Masonry Wall Buildings: Basic Procedures Manual*, Federal Emergency Management Agency, Washington DC, USA, 1998.

[48] G. Yang, H. Z. Liu, K. Zhu, and D. S. Liu, "The inversion analysis for mechanical parameters of dam based on the artificial fish swarm algorithm," *Applied Mechanics and Materials*, vol. 416-417, pp. 1786–1790, 2013.

[49] C. G. Liu, C. S. Gu, and B. Chen, "Zoned elasticity modulus inversion analysis method of a high arch dam based on unconstrained Lagrange support vector regression (support vector regression arch dam)," *Engineering with Computers*, vol. 33, no. 3, pp. 1–14, 2016.

[50] S. A. El-said, A. Osamaa, and A. E. Hassanien, "Optimized hierarchical routing technique for wireless sensors networks," *Soft Computing*, vol. 20, no. 11, pp. 4549–4564, 2015.

[51] E. Hussein, A. I. Hafez, A. E. Hassanien, and A. A. Fahmy, "Nature inspired algorithms for solving the community detection problem," *Logic Journal of the IGPL*, vol. 25, no. 6, pp. 902–914, 2017.

[52] X. Jin, S. Xie, J. He, Y. Lin, Y. Wang, and N. Wang, "Optimization of tuned mass damper parameters for floating wind turbines by using the artificial fish swarm algorithm," *Ocean engineering*, vol. 167, pp. 130–141, 2018.

[53] X. Li, K. Tang, M. N. Omidvar, Z. Yang, and K. Qin, "Benchmark functions for the CEC 2013 special session and competition on large-scale global optimization, CEC 2013," *Gene*, vol. 7, pp. 1–23, 2013.

[54] Y. Wu, X. L. Huang, X. Z. Gao, and K. Zenger, "Cultural artificial fish-swarm optimization algorithm and application in the parameters identification of rotor system," *Electric Machines and Control*, vol. 16, pp. 102–108, 2012.

[55] M. B. Mu'azu, A. T. Salawudeen, T. H. Sikiru, A. Muhammad, and A. I. Abdu, "Weighted artificial fish swarm algorithm with adaptive behavior based linear controller design for nonlinear inverted pendulum," *Journal of Engineering Research*, vol. 20, pp. 1–12, 2015.

[56] E. T. Norouzzadeh, M. Khanmohammadi, and M. Arabpanahan, "Prediction of nonlinear behavior of steel coupling beams under seismic loads based on experimental results," in *Proceedings of 15th World Conference on Earthquake Engineering (15'WCEE)*, vol. 18, Lisbon, Portugal, September 2012.

[57] L. Wang, W. Xuan, N. N. Feng, S. P. Cong, F. Liu, and Q. M. Gao, "Research on seismic performance of reinforced concrete frame with unequal span under low cyclic reversed loading," *The Open Civil Engineering Journal*, vol. 10, no. 1, pp. 373–383, 2016.

[58] C. Corrado and C. Be, "Multi-objective optimization of FRP jackets for improving the seismic response of reinforced concrete frames," *American Journal of Engineering and Applied Sciences*, vol. 9, no. 3, pp. 669–679, 2016.

[59] R. M. Oinam, R. Sugumar, and D. R. Sahoo, "A comparative study of seismic performance of RC frames with masonry infills," *Procedia Engineering*, vol. 173, pp. 1784–1791, 2017.

[60] S. Mazzoni, F. McKenna, M. H. Scott, and G. L. Fenves, *OpenSEES Command Language Manual*, University of California, Berkeley, CA, USA, 2007.

[61] J. B. Mander, M. J. N. Priestley, and R. Park, "Observed stress-strain behavior of confined concrete," *Journal of Structural Engineering*, vol. 114, no. 8, pp. 1827–1849, 1988.

[62] J. B. Mander, M. J. N. Priestley, and R. Park, "Theoretical stress-strain model for confined concrete," *Journal of Structural Engineering*, vol. 114, no. 8, pp. 1804–1826, 1988.

[63] J. Zhao and S. Sritharan, "Modeling of strain penetration effects in fiber-based analysis of reinforced concrete structures," *ACI Structural Journal*, vol. 104, no. 2, pp. 133–141, 2007.